Automated Global Mapping of Minimal Energy Points on Seams of Crossing by the Anharmonic Downward Distortion Following Method: A Case Study of H_2CO

Satoshi Maeda,[†,‡] Koichi Ohno,[*,‡] and Keiji Morokuma[*,†,§]

Department of Chemistry and Cherry L. Emerson Center for Scientific Computation, Emory University, Atlanta, Georgia 30322, Department of Chemistry, Tohoku University, Sendai 980-8578, Japan, and Fukui Institute for Fundamental Chemistry, Kyoto University, Kyoto 606-8103, Japan

Received: December 10, 2008; Revised Manuscript Received: January 2, 2009

Automated global mapping of minimal energy points on seams of crossing (MSX structures) were performed by using the anharmonic downward distortion following (ADD-following) method, which has previously been applied to the single potential energy surfaces (PESs) to perform automated global reaction route mapping. In this study, the ADD-following is applied to a penalty function based on two PESs of different electronic states. The present approach is effective not only for crossing seams between states with different symmetry but also for conical intersections for states with the same symmetry. Many new MSX structures were discovered on the S_0/T_1 and S_1/T_1 crossing seams and the S_0/S_1 conical intersections of H_2CO by automated global mapping using the ADD-following method. A possible pathway for dissociation of formaldehyde excited to S_1 at low energy is discussed.

1. Introduction

Seams of crossing play a key role in mechanisms of photochemical reactions.[1−4] A crossing seam between states with the same symmetry constructs a $(f - 2)$-dimensional hypersurface, called a conical intersection, while the dimension of the seam of crossing for states with different symmetry or spin (neglecting spin−orbit interaction) is $(f - 1)$, where f is the number of vibrational degrees of freedom. Minimal energy structures on seams of crossing (MSX structures) are considered to be critical points for nonadiabatic reactions on the $(f - 2)$- or $(f - 1)$-dimensional hypersurfaces like transition-state (TS) structures on f-dimensional potential energy surfaces (PESs) for normal or adiabatic (single PES) reactions. Hence, characterization of MSX structures is one of the most important tasks in theoretical studies on nonadiabatic reactions, including (but not restricted to) photochemical reactions and some ion−molecule reactions, and optimization techniques of MSX structures have been developed in the past two decades.[5−11] A technique linking conical intersection points has also been developed[11] since internal conversion (IC) can take place at higher energy regions on conical intersection hypersurfaces due to dynamical effects.[12] Nevertheless, an extensive set of MSX structures can be a good starting point to look into such higher energy points on conical intersection hypersurfaces.

Optimization techniques of MSX structures[5−11] have been indispensable tools to conduct investigations on nonadiabatic reaction mechanisms. These techniques can provide one MSX structure starting from an initial guess. In other words, they can be used to confirm whether there is an MSX structure similar to a guessed structure or not. The importance of the MSX structure, once found, in a nonadiabatic reaction can be discussed based on its structure and energy, if a new MSX is found by the optimization. This process requires many trial-and-errors starting from a number of possible guesses, in order not to overlook important MSX structures.

The same sort of problem is known for studies of thermal reaction mechanisms, in which many starting geometries are necessary to locate all or important local equilibrium (EQ) structures and TS structures by an optimization technique.[13,14] Recently, the anharmonic downward distortion following (ADD-following) method was proposed to solve this problem.[15] The ADD-following enables one to find all the routes of reaction starting from an arbitrary EQ structure, which had been impossible by other techniques. A systematic and automatic procedure for finding EQs and TSs by following reaction path networks, i.e., the global reaction route mapping (GRRM) method, has been established[16,17] by using the ADD-following for uphill walks and a standard steepest descent method or its variations[13,14] for downhill walks.

In this paper, an application of the ADD-following method to the problem of automatic global search for MSX structures is reported. We applied the ADD-following method to a penalty function based on energy values of two electronic states proposed by Levine et al.[10] Its performance was tested by applying it to the S_0/S_1, S_0/T_1, and S_1/T_1 crossing seams of H_2CO, and many new MSX structures were discovered for this system by the automated global mapping.

2. Method

2.1. ADD-Following Method. The ADD-following[15−17] was proposed based on a well-known characteristic seen in many typical potential curves (examples of such potential curves are shown in refs 16 and 17). The characteristic is that such a potential curve distorts downward from the harmonic function defined at the bottom of the curve upon approaching a dissociation limit or a TS. Hence, ADD can be a signpost or a compass leading to dissociation channels (DCs) and TS structures from an EQ structure. Actually, traces of ADD maxima starting from EQ structures are very similar to corresponding intrinsic reaction coordinate[18,19] (IRC) pathways integrated from TS structures,[15,16] and the ADD-following in

* To whom correspondence should be addressed. E-mail: ohnok@qpcrkk.chem.tohoku.ac.jp (K.O.); morokuma@emory.edu (K.M.).
† Emory University.
‡ Tohoku University.
§ Kyoto University.

10.1021/jp810898u CCC: $40.75
Published on Web 01/30/2009

combination with a standard downhill walking method from TSs[13,14] has worked successfully in automated global reaction route mapping.[20−25]

The scaled hypersphere search (SHS) method has been developed to detect ADDs in a multidimensional coordinate space.[15−17] The SHS method can find an ADD by a comparison of the reference harmonic function with the actual anharmonic function on the isovalue hypersurface of the harmonic function. The isovalue hypersurface constructs a hyperellipsoid centered at a starting local minimum. In the SHS method, scaled normal coordinates q_i ($=\lambda_i^{1/2}Q_i$) are employed instead of the normal coordinates Q_i, where λ_i is the eigenvalue of Q_i. The use of q_i converts a hyperellipsoidal isovalue surface of the harmonic function into a simple hypersphere. The harmonic energy value on this scaled hypersphere is constant, and hence minima on it correspond to ADD maxima. It follows that an ADD maximal direction can be found by a simple constrained function minimization. By following the ADD maxima with expanding hypersphere radii, reaction pathways can be followed from an EQ to TSs and DCs on single PESs. Further technical details of the ADD-following by the SHS method and the automated GRRM procedure are described in previous papers.[16,17]

This ADD principle may work not only for single PESs but also for some other functions similar to PESs. In this study, it is applied to a penalty function proposed by Levine et al.[10] to search for MSX structures. As shown below, the ADD-following did actually work on the penalty function for H_2CO.

2.2. A Penalty Function. Two values, i.e., an average energy for the target states and an energy gap between the target states, should be minimized simultaneously during the global mapping of MSXs by the ADD-following method. Hence, a natural choice of a form of penalty function should be a sum of these two values with a suitable weight factor. Another requirement for a form of penalty function is that it does not depend on the sign of the energy gap. This requirement is meaningless when two states with the same symmetry are considered, since, for example, the S_1 state is always higher in energy than the S_0 state. However, the sign of $E(S_0) - E(T_1)$ changes depending on the areas of PESs, and the change confuses the automated global mapping code without a special care. A penalty function which satisfies both of these requirements is

$$V(\mathbf{X}) = \frac{E^{\text{state1}}(\mathbf{x}) + E^{\text{state2}}(\mathbf{x})}{2} + \frac{[E^{\text{state1}}(\mathbf{x}) - E^{\text{state2}}(\mathbf{x})]^2}{\alpha} \quad (1)$$

Here, $\mathbf{x}$ is a molecular coordinate with f variables, E^{state1} and E^{state2} are potential energies at $\mathbf{x}$ for the first and second electronic states, and α (>0) is an arbitrary parameter. The gradient vector components and the Hessian matrix components for this function can be obtained as

$$\frac{\partial V(\mathbf{x})}{\partial x_i} = \frac{g_i^{\text{state1}} + g_i^{\text{state2}}}{2} + \frac{2}{\alpha}(E^{\text{state1}} - E^{\text{state2}})(g_i^{\text{state1}} - g_i^{\text{state2}}) \quad (2)$$

and

$$\frac{\partial^2 V(\mathbf{x})}{\partial x_i \partial x_j} = \frac{H_{ij}^{\text{state1}} + H_{ij}^{\text{state2}}}{2} + \frac{2}{\alpha}(g_i^{\text{state1}} - g_i^{\text{state2}})(g_j^{\text{state1}} - g_j^{\text{state2}}) + \frac{2}{\alpha}(E^{\text{state1}} - E^{\text{state2}})(H_{ij}^{\text{state1}} - H_{ij}^{\text{state2}}) \quad (3)$$

respectively, where g_i^{state1} and g_i^{state2} are the ith components of gradient vectors for the first and second electronic states, respectively, and H_{ij}^{state1} and H_{ij}^{state2} are the ith-column jth-row components of Hessian matrices for the first and second electronic states, respectively. This function is very similar to the one introduced by Levine et al.[10] which includes two arbitrary parameters. Since their function is designed for conical intersections between states with the same symmetry, it does not meet the second requirement concerned with the sign of the energy gap. Hence, we modified it as eq 1 to satisfy this requirement. In eq 1, the penalty of the second term is enhanced when the energy difference between the two states is larger than α. On the other hand, minimization of this function gives a converged MSX structure within a desired numerical accuracy when α is small enough.

Penalty function methods[9,10] are not necessarily the best approach for optimizing MSX structures.[26] However, the ADD-following method does not work with constrained optimization techniques[5−8,11] without a special trick. This is because the ADD-following method uses a reference harmonic function defined at a starting minimum point $\mathbf{x}_0$ to detect ADDs in multidimension.[15−17] The reference harmonic function centered at $\mathbf{x}_0$ is no longer meaningful at a different point $\mathbf{x}_1$, since the directions of constraints change depending on the coordinate $\mathbf{x}$. This problem may be solved by updating the reference harmonic function depending on the directions of constraints during the ADD-following, although we use the simpler idea in this study. The same problem will happen when the above penalty function with very small α is employed, because, in the limit of $\alpha = 0$, the second term in eq 1 converges to the delta function which applies rigid constraint in directions lifting the degeneracy of two states as in the case of constrained optimization methods. Hence, our strategy to search for MSX structures by the ADD-following method and the penalty function is composed of two steps: (1) search for candidates of MSX structures which are minima on the penalty function with relatively large α and (2) refinement of such candidate structures by minimizing the penalty function with very small α or by using one of constrained optimization methods.[5−8,11] In this study, we employed the penalty function method[10] also in the second step.

TABLE 1: α Value (in kJ mol^{-1}) Dependence of Geometrical Parameters (in Å or deg), Two Largest Harmonic Frequencies ω_1 and ω_2 (in cm^{-1}), and Energy Gap Δ (in kJ mol^{-1}) between the S_0 and S_1 States at the 3SA-[12e10o]-CASSCF/aug-cc-pVDZ Level, for the MSX of H_2CO Reported in Ref 27[a]

α	R_{C-O}	R_{C-H1}	R_{C-H2}	θ_{O-C-H1}	θ_{O-C-H2}	$\theta_{H1-C-O-H2}$	ω_1	ω_2	Δ
100	1.195	1.107	1.852	143.7	109.3	75.5	3 094	4 453	8.70
50	1.195	1.108	1.856	143.9	109.4	74.8	3 997	6 334	4.31
30	1.194	1.108	1.858	144.0	109.5	74.5	5 078	8 200	2.58
10	1.194	1.108	1.859	144.1	109.5	74.2	8 678	14 236	0.86
1	1.194	1.108	1.860	144.1	109.5	74.1	27 288	45 070	0.09

[a] Also see S_0/S_1-MSX1 in Figure 1.

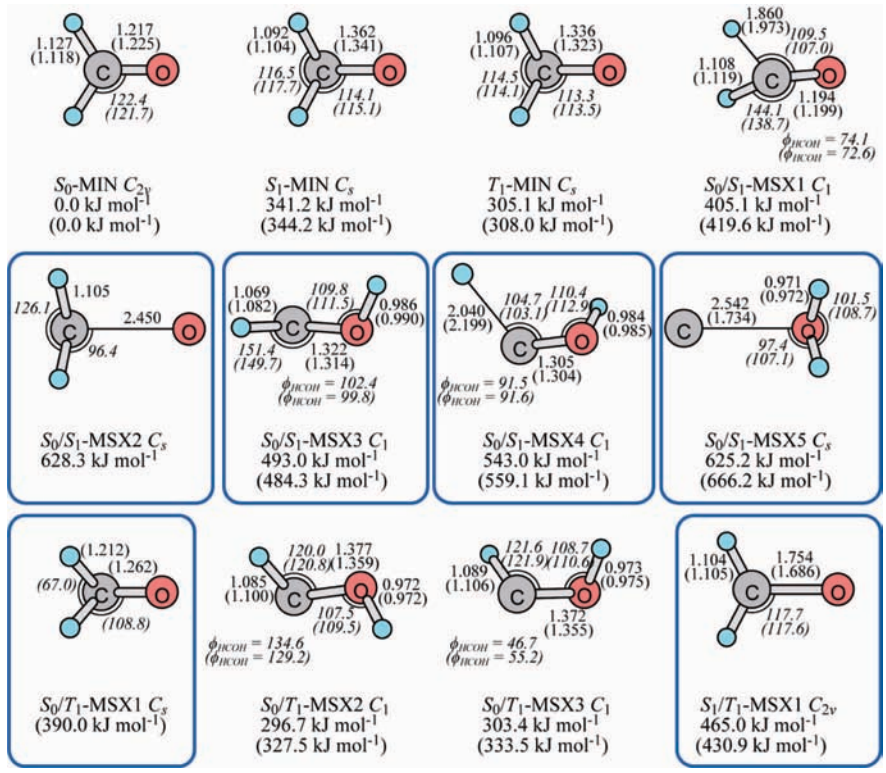

Figure 1. Equilibrium structures on the S_0 (S_0-MIN), S_1 (S_1-MIN), and T_1 (T_1-MIN) potential energy surfaces and MSX structures between the S_0 and S_1 states (S_0/S_1-MSXn), between the S_0 and T_1 states (S_0/T_1-MSXn), and between the S_1 and T_1 states (S_1/T_1-MSXn) of H_2CO. Bond distances (in Å), bond angles and dihedral angles (in deg) with italic, relative energy values (in kJ mol^{-1}), and structure symmetry are also shown. Quantities with and without parentheses are obtained by the CASPT2 method and the CASSCF method, respectively, with the aug-cc-pVDZ basis set and an (12e/10o) active space. Structures newly found in this study are shown with (blue) squares.

Table 1 shows the α value dependence of structure parameters, the two largest harmonic frequencies (ω_1 and ω_2), and the energy gap between the S_0 and S_1 states for an MSX of H_2CO reported by Araujo et al.[27] recently. Since the structure with $\alpha = 1.0$ kJ mol^{-1} has an energy gap of less than 0.1 kJ mol^{-1}, it can be a reference of this computation level. As seen in this table, the structure smoothly converges to the one with $\alpha = 1.0$ kJ mol^{-1}. On the other hand, ω_1 and ω_2 are very large for small α cases, since their eigenvectors correspond to directions lifting the degeneracy of the S_0 and S_1 states in the first order.[1,2] These directions change during the ADD-following, and searches using small α values did not give fruitful results, giving few MSX candidates. Finally, $\alpha = 30$ kJ mol^{-1} was found to be the smallest (best) choice to give enough numbers of MSX candidates for the present system. Although this α value seems to be working in other small organic molecules, some adjustments might be required in the future for different systems such as organometallic systems, cluster systems, and molecules in an environment.

The procedure of applying the ADD-following method to the penalty function is almost the same as the version of the ADD-following for single PESs[15−17] in which only EQ search is performed and saddle-point optimization is skipped, as was adopted to some hydrogen-bonding (H-bond) cluster systems.[28−31] Step lengths are limited to avoid convergence error of CASSCF due to large changes in molecular orbitals induced by a large displacement as its recent application to a single PES of CASSCF theory.[25]

2.3. Computations. In this study, we made two modifications on the GRRM program.[15−17] One is an implementation of the MSX search code, and the other is an addition of an interface with the MOLPRO program package.[32] All geometry changes were treated by the GRRM program, and the electronic energies and gradient vectors were computed by the MOLPRO program. All MSX structures of H_2CO were optimized at the CASSCF[33,34] and CASPT2[35,36] levels with the aug-cc-pVDZ basis set and an active space including 12 electrons and 10 orbitals, i.e., (12e/10o)-CASSCF. In the CASSCF calculations, the three-state averaging (SA3) was performed with equal weight for the S_0, S_1, and T_1 states. In the CASPT2 calculations for the singlet states, the multistate CASPT2 method[36] for the S_0 and S_1 states was employed. On the other hand, the T_1 state was treated by the single-state CASPT2 method.[35] The level shift of 0.2 was applied in the CASPT2 calculations to avoid the intruder state problems in excited-state calculations.[37] The α value in eq 1 was reduced until the energy gap between two states became smaller than 0.1 kJ mol^{-1}.

It is not very practical to use a high-level ab initio method in the initial automated search for MSX candidates, since it requires a large number of force calculations as shown below. Use of a low-level method in the search and a high-level method in the refinement calculation should be the candidate for being the most efficient way. Hence, the 3SA-(4e/3o)-CASSCF/6-31G and 3SA-(2e/3o)-CASSCF/6-31G levels were considered in the initial search. A single use of such a limited active space method may be insufficient, since the (4e/3o) and (2e/3o) will give poor results in LUMO/LUMO+1 quasi-degenerate and HOMO/HOMO−1 quasi-degenerate regions, respectively; these two sets of active space can cover these defects for each other. Some special care will be required in high-symmetry species such as linear molecules since more than one pair of orbitals can be degenerate simultaneously, although it is not necessary for most

of organic molecules with a low symmetry such as C_{2v}, C_s, and C_1.

An automated search using the CASSCF theory stopped frequently because of the SCF convergence problem in some preliminary test calculations. The convergence error can be avoided by reconstruction of an orbital guess by using a different weight for the state average, by including the larger number of states in the state average, or by expanding the active space. Then, a CASSCF calculation starting from such a good orbital guess often gave a converged result for the original set of the weight, the state number, and the active space. The GRRM program applies such trials automatically based on an input when the convergence problem occurs, and the automated searches have never stopped before the completion of the global mapping in the present applications to H_2CO. There has been another problem concerned with the SCF calculations that an electronic structure which has been computed as a low-lying target state changes into a higher state during the global search due to chemical bond rearrangements. Hence, orbital guesses were reconstructed at every predictor (sphere-expansion) step of the ADD-following (uphill) and every 10 steps in IRC-following (downhill) by the 5SA-(6e/6o)-CASSCF calculation, where the S_0, S_1, S_2, T_1, and T_2 states were averaged equally. This procedure works for detection of exchanges of states and/or orbitals induced by a large geometry change, and the subsequent 3SA-(4e/3o or 2e/3o)-CASSCF calculation starting from the 5SA-(6e/6o)-MO guess often converged to the correct S_0, S_1, and T_1 states at these computational levels. In other words, the eigenvalue of the higher state is computed with the larger active space to pick up desired two PESs at a given computation level as is the case for the MO stability check[38,39] for the ground-state PES.

3. Results and Discussion

The S_0 PES of H_2CO has been studied extensively by theoretical calculations[40−51,15−17,20,25] in connection with experimental studies on the unimolecular photodissociation reaction of formaldehyde,[52−57] while there are relatively small numbers of studies on its T_1 and S_1 PESs.[58−63,27] Moore et al.[55] showed that the dissociation occurs on the S_0 PES after rapid IC from the S_1 PES. However, MSX structures for H_2CO reported hitherto are an S_0/S_1-MSX which is located outside the potential well of formaldehyde[27] and an S_0/T_1-MSXs in the potential well of hydroxymethylene (HCOH).[60,62,63] Therefore, a thorough search for MSX structures among the S_0, T_1, and S_1 PESs is of practical importance as well as it is a simple and good example to test whether the ADD-following can discover unknown MSX structures systematically and automatically.

Figure 1 shows three EQ structures on the S_0, S_1, and T_1 PESs and nine MSX structures obtained in this study. Among these nine, five are MSXs between the S_0 and S_1 PESs (S_0/S_1-MSX*n*), three are MSXs between the S_0 and T_1 PESs (S_0/T_1-MSX*n*), and S_1/T_1-MSX1 is an MSX between the S_1 and T_1 PESs. Only the CASSCF structure and energy are shown for S_0/S_1-MSX2 since it has dissociated into $CH_2 + O$ during the optimization at the CASPT2 level. Although optimization of S_0/T_1-MSX1 at the CASSCF level did not converge resulting in dissociation of one of the H atoms, it was confirmed to be an MSX structure at the higher CASPT2 and MRCISD(Q)/aug-cc-pVTZ levels. This S_0/T_1-MSX1 structure obtained with the MRCISD(Q) level has been discussed in our previous paper[64] to be a key structure in photodissociation mechanism and dynamics of formaldehyde. As stated above, only S_0/S_1-MSX1,[27] S_0/T_1-MSX2,[60,62,63] and S_0/T_1-MSX3[60,62,63] have been known, and others are new MSX structures discovered in this study by the automated global mapping.

Figure 2 schematically illustrates the potential profiles for inside the potential wells of formaldehyde and hydroxymethylene based on calculations at the CASPT2 level, where EQs and TSs on the S_1 and T_1 PESs were reoptimized at the CASPT2 level starting from the structures reported in refs 60 and 64.

In spite of great previous efforts, the mechanism of photodissociation dynamics of the formaldehyde molecule, in particular the mechanism of IC from S_1 to S_0, which was suggested by experimental studies to take place before dissociation on S_0,[55] has been unknown. The present results suggests that the photodissociation reaction at low excitation energy ($<32\,000$ $cm^{-1} = 383$ kJ mol^{-1}) from S_1 passes through the T_1 state. The direct $S_1 \rightarrow S_0$ transition through the lowest S_0/S_1-MSX1 is reachable only after going over the barrier (438 kJ mol^{-1}) at the S_1 TS that leads to the H + HCO dissociation. The direct $S_1 \rightarrow S_0$ transition via any other newly found S_0/S_1-MSX requires too high energy (>480 kJ mol^{-1}). Thus no direct $S_1 \rightarrow S_0$ transition is likely to take place at lower excitation energy. The $S_1 \rightarrow T_1$ transition via the newly found S_1/T_1-MSX1 in the basin of S_1-MIN also requires high energy (431 kJ mol^{-1}). However, the $S_1 \rightarrow T_1$ transition may be able to take place by trickling down from S_1 to T_1 at all the geometries, while the molecule in the S_1 state spends a long time oscillating around the S_1-MIN structure,[64] because PESs for the S_1 and T_1 states are very close and nearly parallel to each other in energy at any place in the basin of S_1-MIN. Although the probability at each geometry may be small because the spin−orbital coupling between the two states belonging to the same electronic configuration is expected to be small, the integrated probability over a long time could be substantial. Once the system comes down to T_1 in the S_1-MIN basin, the $T_1 \rightarrow S_0$ transition via the newly found S_0/T_1-MSX1 (390 kJ mol^{-1}) can take place inside this H_2CO basin. There are two other lower energy S_0/T_1-MSXs ($\sim$330 kJ mol^{-1}) located on the HCOH side; however, they are reachable only after going over the T_1 TS for isomerization with a high energy of 465 kJ mol^{-1} and are not likely to be important for the transition of T_1 formed from S_1 at low excitation energy to S_0.[55] The present conclusion based on the CASPT2 energetics is consistent with the result obtained recently by us based on MRCISD(Q)/AV5Z energetics.[64] After the transition to S_0, the dynamics on the S_0 PES should start in the H_2CO basin and propagate via the tight-TS or the roaming pathway to give the $H_2 + CO$ product.[56] Surface-hopping trajectory simulations[65] will be required in the future to further confirm this $S_1 \rightarrow T_1 \rightarrow S_0$ transition mechanism with computations of the excited-state lifetimes.

Two recently reported MSXs, S_0/T_1-MSX2 and S_0/T_1-MSX3,[60,62,63] are placed along the internal rotation coordinate of hydroxymethylene as shown in Figure 2B. However, some MSXs are located at points strongly deviated from a specific reaction coordinate, and they are very difficult to be guessed. For example, the crossing for S_1/T_1-MSX1 cannot be expected based on a dissociation reaction into $CH_2 + O$. According to spectroscopic data,[66,67] PESs of the S_0, S_1, and T_1 states correlate with CH_2 (X^3B_1) + O (^3P), CH_2 (a^1A_1) + O (^1D), and CH_2 (a^1A_1) + O (^3P), respectively, where CH_2 (a^1A_1) + O (^1D) and CH_2 (a^1A_1) + O (^3P) are higher in energy than CH_2 (X^3B_1) + O (^3P) by 19 015 cm^{-1} and 3147 cm^{-1}, respectively. Hence, the S_1 PES is expected to be always above the T_1 PES along a minimum energy path of the DC into $CH_2 + O$. The change in the coordination direction of the O atom toward CH_2 and the increase of the HCH bond angle help to achieve the degeneracy

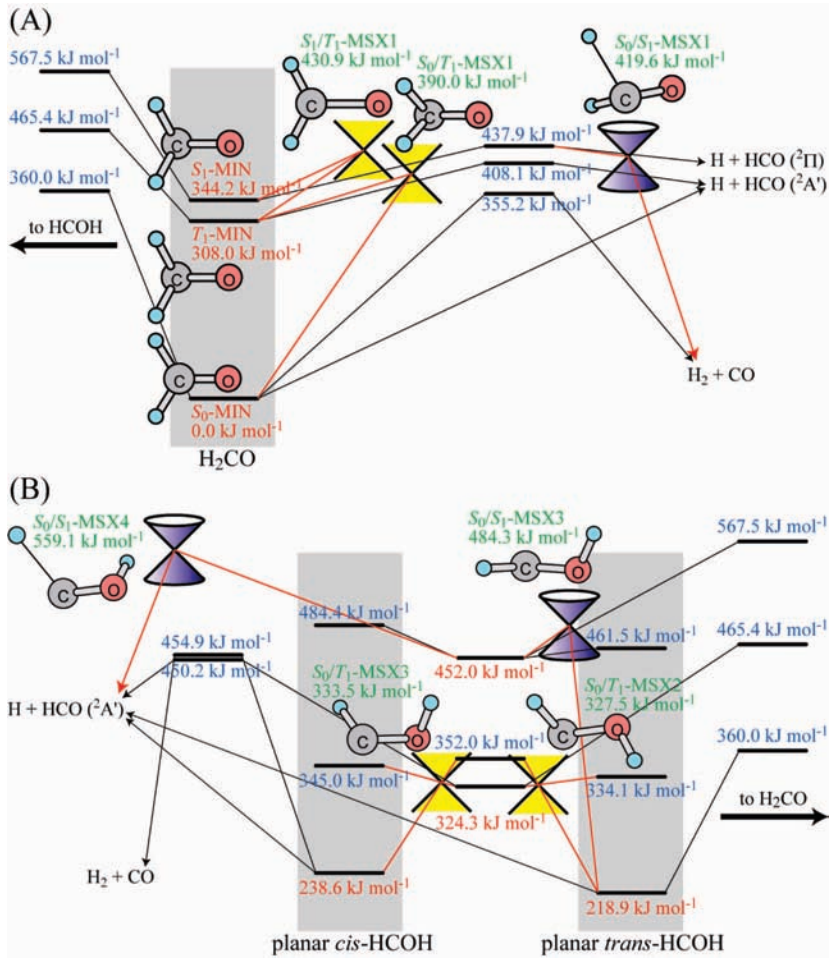

Figure 2. Illustration of the potential energy profiles for inside the potential wells of formaldehyde (A) and hydroxymethylene (B) based on the CASPT2 theory. Connections related to the MSX structures in Figure 1 are shown with red lines.

at the S_1/T_1-MSX1 structure. The S_0/T_1-MSX1 structure is also difficult to be guessed, since there has been no report of an IRC pathway as well as a minimum energy path of DC which passes through a structure like S_0/T_1-MSX1 for all of the S_0, S_1, and T_1 PESs. This may be the reason why these very important MSXs have been unknown. The present approach will be a great help to find out such difficult MSXs systematically.

In the initial automated search by the ADD-following method, 8 MSX candidate structures were obtained for S_0/S_1-MSX at the (2e/3o)-CASSCF level and 10 at the (4e/3o)-CASSCF level; at the refined optimization, these resulted in 5 unique S_0/S_1-MSX structures in Figure 1. In the S_0/T_1-MSX search 8 (2e/3o)-CASSCF and 4 (4e/3o)-CASSCF candidate structures resulted in 3 S_0/T_1-MSX structures, and 1 (2e/3o)-CASSCF and 2 (4e/3o)-CASSCF candidates resulted in 1 refined S_1/T_1-MSX structure in Figure 1. Although the extensive systematic refined search located smaller numbers of MSX structures, the extra cost for starting from larger numbers of candidate structures should be meaningful to confirm that there is no other significant MSX structure between the set of two states. Computation cost, i.e., the number of gradient evaluations for the initial automated search by the ADD-following method, is very large (as in its previous applications to single PES); 37 418 gradient calculations were needed for the S_0/S_1-MSX search at the (2e/3o)-CASSCF level, 53 720 at the (4e/3o)-CASSCF level, 37 210 for the S_0/T_1-MSX search at the (2e/3o)-CASSCF level, 22 412 at the (4e/3o)-CASSCF level, 3035 for the S_1/T_1-MSX search at the (2e/3o)-CASSCF level, and 8851 at the (4e/3o)-CASSCF level. The numbers of gradient calculations linearly depend on the numbers of local minima since the ADD-following should start from all obtained local minima in the global mapping. The average number of force calculations for one local minimum on the present penalty function of H_2CO is 4929, which is larger than that on the single PES of H_2CO of 3597.[25] This is because the 4929 includes costs of numerical Hessian evaluations via 24 force differentiation, while 247 Hessians were computed analytically for each local minimum on average in the case of the single PES of H_2CO.[25] Hence, we conclude that the performance of the ADD-following method on the penalty function of H_2CO is comparable to the case of the single PES of H_2CO.

It should be noted that a probability of overlooking MSX structures in an automated global mapping may be higher than the case of global reaction route mapping on ground-state PES, since results of excited-state calculations strongly depend on a choice of an active space, a basis set, dynamical correlations, and others. For example, the S_0/T_1-MSX1 structure was overlooked if we considered only the (12e/10o)-CASSCF method in the present refinement calculations. Although this problem can be avoided if one used a very high level method from the initial automated search, it is not practical because of numerous force calculations required for automated global mapping as shown above. Hence, it is better to consider more than one practical computation level in both initial automated search and final refinement calculation to reduce the probability of overlooking important MSX structures.

4. Remarks on Applications to Larger Systems

In this study, we treated all ADDs starting from all local minima obtained on the penalty function; i.e., the full-ADD-following method is employed. Although the full-ADD-following is very expensive, it is very powerful to locate almost all structures including very high energy ones for a given computational level.[15−17,20−25] Recently, the large-ADD-following method was introduced to quickly explore low-energy regions connected via low barriers,[28] and it has been applied to relatively large systems such as H-bond cluster systems with ca. 30 atoms[28−31] and an organometallic system with about 100 atoms[68,69] coupled with the ONIOM method.[70−73] In other words, the large-ADD-following can be effective for low-barrier processes such as H-bond rearrangements, efficient catalytic processes in mild conditions, and internal rotations. Photoinduced internal rotation is very important in some biological systems,[1,4] and test applications of the large-ADD-following method to such model systems are in progress. An interface with the ONIOM method is also under development.

5. Conclusion

An application of the ADD-following method[15−17] to the problem of searching MSX structures automatically and systematically was reported. The ADD-following method was applied to a penalty function[10] based on potential energy values of two electronic states. The performance of the ADD-following method on the penalty function of H_2CO was similar to that of the single (ground-state) PES of H_2CO, and many new MSX structures were obtained automatically on the S_0/S_1, S_0/T_1, and S_1/T_1 crossing seams of H_2CO. The ADD-following method can be a powerful tool to systematically search for MSX structures, as it has been so for global reaction route mapping on single PESs.

Acknowledgment. S.M. thanks Dr. Marcus Lundberg, Dr. Lung Wa Chung, Dr. Zhi Wang, and Dr. Peng Zhang for their helpful comments on excited-state calculations. S.M. is supported a by Research Fellowship of the Japan Society for Promotion of Science for Young Scientists. This work is partly supported by the Japan Science and Technology Agency with a Core Research for Evolutional Science and Technology (CREST) grant in the Area of High Performance Computing for Multiscale and Multiphysics Phenomena.

References and Notes

(1) Bernardi, F.; Olivucci, M.; Robb, M. A. *Chem. Soc. Rev.* **1996**, *25*, 321.
(2) Yarkony, D. R. *Acc. Chem. Res.* **1998**, *31*, 511.
(3) Sobolewski, A. L.; Domcke, W.; Dedonder-Lardeux, C.; Jouvet, C. *Phys. Chem. Chem. Phys.* **2002**, *4*, 1093.
(4) Levine, B. G.; Martínez, T. J. *Annu. Rev. Phys. Chem.* **2007**, *58*, 613.
(5) Koga, N.; Morokuma, K. *Chem. Phys. Lett.* **1985**, *119*, 371.
(6) Manaa, M. R.; Yarkony, D. R. *J. Chem. Phys.* **1993**, *99*, 5251.
(7) Bearpark, M. J.; Robb, M. A.; Schlegel, H. B. *Chem. Phys. Lett.* **1994**, *223*, 269.
(8) Anglada, J. M.; Bofill, J. M. *J. Comput. Chem.* **1997**, *18*, 992.
(9) Ciminelli, C.; Granucci, G.; Persico, M. *Chem. Eur. J.* **2004**, *10*, 2327.
(10) Levine, B. G.; Coe, J. D.; Martínez, T. J. *J. Phys. Chem. B* **2008**, *112*, 405.
(11) Sicilia, F.; Blancafort, L.; Bearpark, M. J.; Robb, M. A. *J. Chem. Theory Comput.* **2008**, *4*, 257.
(12) Migani, A.; Robb, M. A.; Olivucci, M. *J. Am. Chem. Soc.* **2003**, *125*, 2804.
(13) Schlegel, H. B. *J. Comput. Chem.* **2003**, *24*, 1514.
(14) Jensen, F. *Introduction to Computational Chemistry*, 2nd. ed.; Wiley: Chichester, 2007.
(15) Ohno, K.; Maeda, S. *Chem. Phys. Lett.* **2004**, *384*, 277.
(16) Maeda, S.; Ohno, K. *J. Phys. Chem. A* **2005**, *109*, 5742.
(17) Ohno, K.; Maeda, S. *J. Phys. Chem. A* **2006**, *110*, 8933.
(18) Fukui, K. *Acc. Chem. Res.* **1981**, *14*, 363.
(19) Ishida, K.; Morokuma, K.; Komornicki, A. *J. Chem. Phys.* **1977**, *66*, 2153.
(20) Ohno, K.; Maeda, S. *Phys. Scr.* **2008**, *78*, 058122.
(21) Yang, X.; Maeda, S.; Ohno, K. *J. Phys. Chem. A* **2005**, *109*, 7319.
(22) Yang, X.; Maeda, S.; Ohno, K. *Chem. Phys. Lett.* **2006**, *418*, 208.
(23) Yang, X.; Maeda, S.; Ohno, K. *J. Phys. Chem. A* **2007**, *111*, 5099.
(24) Watanabe, Y.; Maeda, S.; Ohno, K. *Chem. Phys. Lett.* **2007**, *447*, 21.
(25) Maeda, S.; Ohno, K. *Chem. Phys. Lett.* **2008**, *460*, 55.
(26) Keal, T. W.; Koslowski, A.; Thiel, W. *Theor. Chem. Acc.* **2007**, *118*, 837.
(27) Araujo, M.; Lasorne, B.; Bearpark, M. J.; Robb, M. A. *J. Phys. Chem. A* **2008**, *112*, 7489.
(28) Maeda, S.; Ohno, K. *J. Phys. Chem. A* **2007**, *111*, 4527.
(29) Luo, Y.; Maeda, S.; Ohno, K. *J. Phys. Chem. A* **2007**, *111*, 10732.
(30) Maeda, S.; Ohno, K. *J. Phys. Chem. A* **2008**, *112*, 2962.
(31) Luo, Y.; Maeda, S.; Ohno, K. *J. Comput. Chem.*, DOI: 10.1002/jcc.21117.
(32) Werner, H.-J.; Knowles, P. J.; Lindh, R.; Manby, F. R.; Schütz, M.; Celani, P.; Korona, T.; Mitrushenkov, A.; Rauhut, G.; Adler, T. B.; Amos, R. D.; Bernhardsson, A.; Berning, A.; Cooper, D. L.; Deegan, M. J. O.; Dobbyn, A. J.; Eckert, F.; Goll, E.; Hampel, C.; Hetzer, G.; Hrenar, T.; Knizia, G.; Köppl, C.; Liu, Y.; Lloyd, A. W.; Mata, R. A.; May, A. J.; McNicholas, S. J.; Meyer, W.; Mura, M. E.; Nicklass, A.; Palmieri, P.; Pflüger, K.; Pitzer, R.; Reiher, M.; Schumann, U.; Stoll, H.; Stone, A. J.; Tarroni, R.; Thorsteinsson, T.; Wang, M.; Wolf, A. MOLPRO, version 2008.1, a package of ab initio programs; see http://www.molpro.net.
(33) Werner, H.-J.; Knowles, P. J. *J. Chem. Phys.* **1985**, *82*, 5053.
(34) Knowles, P. J.; Werner, H.-J. *Chem. Phys. Lett.* **1985**, *115*, 259.
(35) Werner, H.-J. *Mol. Phys.* **1996**, *89*, 645.
(36) Finley, J.; Malmqvist, P.-Å.; Roos, B. O.; Serrano-Andreś, L. *Chem. Phys. Lett.* **1998**, *288*, 299..
(37) Roos, B. O.; Andersson, K. *Chem. Phys. Lett.* **1995**, *245*, 215.
(38) Seeger, R.; Pople, J. A. *J. Chem. Phys.* **1977**, *66*, 3045.
(39) Bauernschmitt, R.; Ahlrichs, R. *J. Chem. Phys.* **1996**, *104*, 9047.
(40) Jaffe, R. L.; Hayes, D. M.; Morokuma, K. *J. Chem. Phys.* **1974**, *60*, 5108.
(41) Hernandez, J. A.; Carbo, R. *J. Chim. Phys. Pcb.* **1975**, *72*, 959.
(42) Jaffe, R. L.; Morokuma, K. *J. Chem. Phys.* **1976**, *64*, 4881.
(43) Goddard, J. D.; Schaefer, H. F., III *J. Chem. Phys.* **1979**, *70*, 5117.
(44) Scuseria, G. E.; Schaefer, H. F., III *J. Chem. Phys.* **1989**, *90*, 3629.
(45) Deng, L.; Ziegler, T.; Fan, L. *J. Chem. Phys.* **1993**, *99*, 3823.
(46) Bondensgård, K.; Jensen, F. *J. Chem. Phys.* **1996**, *104*, 8025.
(47) Nakano, H.; Nakayama, K.; Hirao, K.; Dupuis, M. *J. Chem. Phys.* **1997**, *106*, 4912.
(48) Jensen, F. *Theor. Chem. Acc.* **1998**, *99*, 295.
(49) Quapp, W.; Hirsch, M.; Imig, O.; Heidrich, D. *J. Comput. Chem.* **1998**, *19*, 1087.
(50) Feller, D.; Dupuis, M.; Garrett, B. C. *J. Chem. Phys.* **2000**, *113*, 218.
(51) Harding, L. B.; Klippenstein, S. J.; Jasper, A. W. *Phys. Chem. Chem. Phys.* **2007**, *9*, 4055.
(52) Gelbart, W. M.; Elert, M. L.; Heller, D. F. *Chem. Rev.* **1980**, *80*, 403.
(53) Clouthier, D. J.; Ramsey, D. A. *Annu. Rev. Phys. Chem.* **1983**, *34*, 31.
(54) Moore, C. B.; Weisshaar, J. C. *Annu. Rev. Phys. Chem.* **1983**, *34*, 525.
(55) Green, W. H., Jr.; Moore, C. B.; Polik, W. F. *Annu. Rev. Phys. Chem.* **1992**, *43*, 591..
(56) Townsend, D.; Lahankar, S. A.; Lee, S. K.; Chambreau, S. D.; Suits, A. G.; Zhang, X.; Rheinecker, J.; Harding, L. B.; Bowman, J. M. *Science* **2004**, *306*, 1158.
(57) Moore, C. B. *Annu. Rev. Phys. Chem.* **2007**, *58*, 1.
(58) Yamaguchi, Y.; Wesolowski, S. S.; Van Huis, T. J.; Schaefer, H. F., III *J. Chem. Phys.* **1998**, *108*, 5281.
(59) Beack, K. K. *J. Chem. Phys.* **2000**, *112*, 1.
(60) Zhang, P. Ph.D. Thesis, Emory Universitry, 2005.
(61) Simonsen, J. B.; Rusteika, N.; Johnson, M. S.; Sølling, T. I. *Phys. Chem. Chem. Phys.* **2008**, *10*, 674.
(62) Shepler, B. C.; Epifanovsky, E.; Zhang, P.; Bowman, J. M.; Krylov, A. I.; Morokuma, K. *J. Phys. Chem. A* **2008**, *112*, 13267.
(63) Manohar, P. U.; Krylov, A. I. *J. Chem. Phys.*, submitted for publication.
(64) Zhang, P.; Maeda, S.; Morokuma, K.; Braams, B. J. *J. Chem. Phys.*, in press.
(65) Tully, J. C. *J. Chem. Phys.* **1990**, *93*, 1061.
(66) http://webbook.nist.gov.
(67) http://physics.nist.gov.
(68) Maeda, S.; Ohno, K. *J. Phys. Chem. A* **2007**, *111*, 13168.

(69) Maeda, S.; Ohno, K. *J. Am. Chem. Soc.* **2008**, *130*, 17228.
(70) Svensson, M.; Humbel, S.; Froese, R. D. J.; Matsubara, T.; Sieber, S.; Morokuma, K. *J. Phys. Chem.* **1996**, *100*, 19357.
(71) Dapprich, S.; Komáromi, I.; Byun, K. S.; Morokuma, K.; Frisch, M. J. *THEOCHEM* **1999**, *1*, 461–462.
(72) Morokuma, K. *Bull. Korean Chem. Soc.* **2003**, *24*, 797.
(73) Vreven, T.; Byun, K. S.; Komáromi, I.; Dapprich, S.; Montgomery, J. A., Jr.; Morokuma, K.; Frisch, M. J. *J. Chem. Theory Comput.* **2006**, *2*, 815.

JP810898U